

Modified relaxation time Monte Carlo method for continuum-transition gas flows

Xudong Lan, Jun Sun, Zhixin Li*

*Key Laboratory of Thermal Science and Power Engineering of Education Ministry, School of Aerospace,
Tsinghua University, Beijing 100 084, PR China*

Received 24 September 2007; received in revised form 15 January 2008; accepted 16 January 2008
Available online 26 January 2008

Abstract

Gas flows in the continuum-transition regime often occur in micro-electro-mechanical systems. The relaxation time Monte Carlo (RTMC) method was modified by using an ellipsoid statistical model and a multiple translational temperature model in the BGK model equation to simulate continuum-transition gas flows. The modified RTMC method uses a simplified form of the generalized relaxation time, which is related to the macro velocity and the local Knudsen number. The results for Couette flow and Poiseuille flow in microchannels predicted using the modified RTMC and the DSMC are in good agreement with the modified RTMC being much faster than the DSMC for continuum-transition gas flow simulations.

© 2008 Elsevier Inc. All rights reserved.

Keywords: Modified RTMC; Micro gas flow; Continuum-transition regime; BGK model equation

1. Introduction

Flow regimes are classified according to the Knudsen number (Kn) which is defined as the ratio of the molecular mean free path to a characteristic length of the system [1,2]. In the continuum flow regime ($Kn < 0.001$) and the slip flow regime ($0.001 < Kn < 0.1$), the Navier–Stokes equations with appropriate boundary conditions are sufficient to describe the flow behavior. For high Kn gas flows ($Kn > 1$), the Boltzmann equation with appropriate boundary conditions can be solved theoretically and numerically with some assumptions [3]. For gas flows in the continuum-transition regime ($0.01 < Kn < 1$), the Navier–Stokes equations are not sufficient to predict the flow characteristics accurately due to rarefaction effects. In addition, the advantage of the pure particle based methods is lost due to the high computational cost. Therefore, accurate models reliable and low cost are needed for the continuum-transition regime.

The direct simulation Monte Carlo (DSMC) method established by Bird [1] is the most successful method for numerical predictions of rarefied gas flows. However, micro-electro-mechanical systems

* Corresponding author. Tel.: +86 10 6277 2919.
E-mail address: lizhx@tsinghua.edu.cn (Z. Li).

(MEMS) often have gas flows in the continuum-transition regime with high densities due to the small characteristic length. The DSMC method suffers from statistical scattering and high computational cost due to the frequent molecular collisions. Pullin [4] proposed a particle-based continuum method called the equilibrium particle simulation method (EPSM) to simulate high density ideal gas flows. He assumed that the molecules were in local equilibrium at each time step and simulated the collision effects by redistributing the momentum and energy of all the particles in each cell to simulate the collisions between particles. Chen et al. [5] constructed a hybrid method combining the EPSM with the DSMC to simulate continuum-transition and transition flows. Macrossan [6–8] developed the EPSM method based on the BGK model equation and proposed the relaxation time simulation method (RTSM). The RTSM does not redistribute all the particles in each cell, but only a selected number of particles according to the local relaxation time, which is associated with the local density, temperature and viscosity. To overcome some limitations of the EPSM and RTSM methods, Wang [9] proposed a new method called the relaxation time Monte Carlo (RTMC) method to predict flows in the continuum-transition regime. Wang et al. [10] further developed the RTSM by introducing the Larsen–Borgnakke model with discrete rotational energies to model the energy exchange between the translational and internal modes.

However, most of these methods have been based on the BGK model equation with the Maxwellian distribution and a Prandtl number (Pr) of unity. Holway [11] introduced an anisotropic Gaussian distribution to replace the Maxwellian (isotropic Gaussian) distribution in the BGK model equation and suggested the ellipsoid-statistical (ES) model for the effect of the Prandtl number. Zhang et al. [12] developed the ES model and proved the existence and uniqueness of the solution for the ES-BGK model equation mathematically for $Pr \in [2/3, \infty)$. Recently, Xu and Josyula [13] and Xu and Liu [14,15] introduced a new model called the multiple translational temperature (MTT) model to replace the Maxwellian distribution function in the BGK model equation and defined a generalized relaxation time. Xu's MTT model was verified to be more efficient than microscopic methods for predicting non-equilibrium shock structures, Couette and Poiseuille flows, nonlinear heat conduction problems and unsteady Rayleigh problems.

In this paper, the RTMC method is further modified by introducing the ES model or the MTT model and a simplified generalized relaxation time into the BGK model equation. The model is validated by numerical simulations of continuum-transition gas flows in microchannels, such as micro Couette flows and micro Poiseuille flows. The computational time consumed by the modified RTMC method with the MTT model is compared with that of the DSMC method.

2. BGK model equation

2.1. Analysis of Boltzmann equation

The Boltzmann equation derived from the Liouville equation [3] is usually used to describe rarefied gas flows and micro gas flows with high Knudsen numbers. The Boltzmann equation is

$$\frac{\partial f}{\partial t} + \mathbf{u} \cdot \frac{\partial f}{\partial \mathbf{r}} + \mathbf{F} \cdot \frac{\partial f}{\partial \mathbf{u}} = \left(\frac{\partial f}{\partial t} \right)_{\text{coll}} \quad (1)$$

where f is the distribution function, \mathbf{u} is the velocity vector, $\mathbf{u} \cdot \partial f / \partial \mathbf{r}$ is the convection term, \mathbf{F} is the external force and $(\partial f / \partial t)_{\text{coll}}$ is the collision term which equals $\int_{-\infty}^{\infty} \int_0^{4\pi} (f' f'_1 - f f_1) c_r \sigma d\Omega dc_1$. A detailed description of the collision term was given by Bird [1].

Many numerical methods have been developed from the Boltzmann equation, such as the moment method [16,17], particle based method (DSMC, MD, etc.) [1] and the model equation [18]. These methods have been widely used in scientific research and engineering applications. However, there are few analyses of simplification of the Boltzmann equation. The dimensionless variables in the Boltzmann equation are

$$\begin{cases} \hat{t} = t/t_0 \\ \hat{\mathbf{u}} = \mathbf{u}/\mathbf{u}_0 \\ \hat{\mathbf{r}} = \mathbf{r}/L \end{cases} \quad (2)$$

where t_0 is the characteristic time, \mathbf{u}_0 is the molecular mean velocity vector and L is the characteristic length of the calculational region.

Additionally, from dimensional analysis, there are

$$\begin{cases} \int_0^{4\pi} \sigma \, d\Omega \sim d^2, \\ \int_{-\infty}^{\infty} (f^* f_1^* - ff_1) c_r \, dc_1 \sim f n v_0, \\ (\partial f / \partial t)_{\text{coll}} \sim n d^2 v_0 f, \\ n d^2 \sim 1 / \lambda \end{cases} \quad (3)$$

where d is the molecular diameter and λ is the molecular mean free path. Therefore,

$$\left(\frac{\partial f}{\partial t} \right)_{\text{coll}} = J(ff_1) = \hat{J}(ff_1) \frac{v_0}{\lambda} \quad (4)$$

Neglecting external forces and substituting Eq. (4) into the Boltzmann equation, Eq. (1) gives

$$\frac{\partial f}{\partial t} + \frac{v_0 t_0}{L} \hat{\mathbf{u}} \cdot \frac{\partial f}{\partial \hat{\mathbf{r}}} = \frac{v_0 t_0}{\lambda} \hat{J}(ff_1) \quad (5)$$

with $Kn = \lambda/L$ and the Strouhal number, $Sh = L/v_0 t_0$, the dimensionless Boltzmann equation is,

$$\frac{\partial f}{\partial \hat{t}} + \frac{1}{Sh} \hat{\mathbf{u}} \cdot \frac{\partial f}{\partial \hat{\mathbf{r}}} = \frac{1}{Kn Sh} \hat{J}(ff_1) \quad (6)$$

The relative significance of each term in the dimensionless Boltzmann equation can then be analyzed as a function of the Knudsen and Strouhal numbers. When Sh is large enough, the convection term can be neglected. If Kn is also large enough, the collision term can be neglected.

The DSMC method, as a particle based method, has been verified to be equivalent to the Boltzmann equation [18]. In the DSMC method, the characteristic velocity v_0 is usually about 10^2 – 10^3 m/s and the characteristic time t_0 can be the calculational time step Δt , which is 10^{-10} – 10^{-11} s in micro gas flows simulation. If the characteristic length $L = 1 \mu\text{m}$, Sh is on the order of 10^2 , which is large enough to neglect the convection term. Here, if Kn is small, such as on the order of 10^{-2} , the product of Kn and Sh is not sufficiently large to neglect the collision term, except for very large Sh due to the large characteristic length. Inversely, when Kn and the characteristic length are both large enough, for example in rarefied gas flows, the convection term should be neglected and the collision term can be replaced by the linear expression in the BGK model. In such situations, a simplified particle method based on the BGK model equation, such as the RTMC method, can be used to more efficiently simulate high Kn gas flows.

2.2. Solution of BGK model equation

The model equation is an approximation of the Boltzmann equation with a simplified collision term. The most famous model equation is the BGK model equation proposed by Bhatnagar, et al. [19]

$$\frac{\partial f}{\partial t} + \mathbf{u} \cdot \frac{\partial f}{\partial \mathbf{r}} + \mathbf{F} \cdot \frac{\partial f}{\partial \mathbf{u}} = \frac{(f^{\text{eq}} - f)}{\tau} \quad (7)$$

where $\tau = \mu/(nkT)$ is the relaxation time, μ is the viscosity, n is the number density, k is the Boltzmann constant, T is the temperature and f^{eq} is the local Maxwellian distribution function.

$$f^{\text{eq}} = (\beta^2/\pi)^{3/2} \exp(-\beta^2 \mathbf{c}'^2) \quad (8)$$

where $\beta = \sqrt{m/2kT}$, m is the molecular mass, $\mathbf{c}' = \mathbf{c} - \mathbf{c}_0$ is the thermal velocity and \mathbf{c} and \mathbf{c}_0 are the molecular and macroscopic velocities.

Generally, by assuming the distribution function f is spatially homogeneous so only changes with time are considered and neglecting the external forces, the BGK model equation can be simplified as,

$$\frac{\partial f}{\partial t} = \frac{f^{\text{eq}} - f}{\tau} \quad (9)$$

By integrating this equation from time t to $t + \Delta t$, the exact solution is

$$f(t + \Delta t) = \exp(-\Delta t/\tau)f(t) + (1 - \exp(-\Delta t/\tau))f^{\text{eq}} \quad (10)$$

where $f(t)$ and $f(t + \Delta t)$ are the distribution functions at time t and $t + \Delta t$, respectively.

The RTMC method presented by Wang [9] was based on Eq. (10). However, as Kn decreases, for example, in the continuum-transition regime in a microchannel, the molecular number density increases. The collision frequency is very high due to the small distance between molecules. Large gradients may occur in some positions in the system, especially for complex geometries. The equilibrium assumption may then fail due to the large gradients. Therefore, the RTMC method must be modified to simulate continuum-transition gas flows.

3. Modified RTMC method

Due to limitations in the Maxwellian distribution function for simulating continuum-transition gas flows, researchers have suggested other models to replace the Maxwellian distribution in the BGK model equation.

3.1. Ellipsoid-statistical (ES) model

The BGK model represents the main characteristics of the collision term in the Boltzmann equation and has been successfully used for rarefied gas flows. However, two major problems restrict the further applications of the BGK model equation. First, relaxation time, τ , in the BGK model is not related to the velocity and second, Pr is always unity.

Holway [11] introduced an anisotropic Gaussian distribution (ellipsoid-statistical, ES) to replace the Maxwellian (isotropic Gaussian) distribution in the BGK model equation. The distribution function for the ES model is,

$$g_{\text{H}} = \frac{\rho}{\sqrt{2\pi\beta_{ij}}} \exp\left(-\frac{1}{2}\beta_{ij}^{-1}\mathbf{c}'_i\mathbf{c}'_j\right) \quad (11)$$

where ρ is the density. The matrix β_{ij} is given by

$$\beta_{ij} = \frac{1}{Pr}RT\delta_{ij} + \left(1 - \frac{1}{Pr}\right)\frac{p_{ij}}{\rho} \quad (12)$$

where β_{ij}^{-1} denotes the inverse matrix, T is the local temperature and p_{ij} is the stress tensor.

For $Pr \in [2/3, \infty)$, Zhang et al. [12] proved the existence and uniqueness of the solution for the ES-BGK model equation and modified the matrix β_{ij} as follows:

$$\beta_{kk}^0 = \left(1 - \frac{Pr-1}{Pr} \exp\left(-\frac{1}{Pr}\frac{t}{\tau}\right)\right)RT^0 + \frac{Pr-1}{Pr} \exp\left(-\frac{1}{Pr}\frac{t}{\tau}\right)\frac{p_{kk}^0}{\rho^0} \quad (13)$$

where the superscript “0” denotes the initial state, $k = 1, 2, 3$ and $\sum_{k=1}^3 p_{kk}^0 = 3\rho^0 RT^0$.

Zhang et al. [12] assumed that $p_{11}^0 \leq p_{22}^0 \leq p_{33}^0$ and $p_{11}^0 = \alpha p_{33}^0$. Here, $0 < \alpha \leq 1$. Therefore,

$$\begin{aligned} \frac{\alpha}{1+\alpha}RT^0 \leq \beta_{33}^0 \leq \beta_{22}^0 \leq \beta_{11}^0 \leq \frac{1}{Pr}RT^0, & \quad \frac{2}{3} \leq Pr < 1 \\ \frac{1}{Pr}RT^0 \leq \beta_{11}^0 \leq \beta_{22}^0 \leq \beta_{33}^0 \leq \frac{3Pr-1}{Pr(1+\alpha)}RT^0, & \quad 1 \leq Pr < \infty \end{aligned} \quad (14)$$

3.2. Multiple translational temperature (MTT) model

Xu et al. [13,14] introduced the multiple translational temperature (MTT) model to replace the Maxwellian distribution function, f^{eq} , in the BGK model equation. For two-dimensional cases, the multiple temperature distribution function is

$$g_{\text{MTT}} = \rho \sqrt{\frac{\lambda_x}{\pi}} \sqrt{\frac{\lambda_y}{\pi}} \sqrt{\frac{\lambda_z}{\pi}} \exp(-\lambda_x(u - U)^2 - \lambda_y(v - V)^2 - \lambda_z w^2) \tag{15}$$

where ρ is the density, U and V are the macroscopic velocities in the x and y directions and (u, v, w) are the components of particle velocities in the x , y and z directions. The parameters $\lambda_x = m/2kT_x$, $\lambda_y = m/2kT_y$, and $\lambda_z = m/2kT_z$ are related to the translational temperatures T_x , T_y and T_z in the x , y and z directions.

3.3. Simplified generalized relaxation time

Xu et al. [15] defined a generalized relaxation time,

$$\tau^* = \frac{\tau}{1 + \tau(D^2 f^{\text{eq}}/Df^{\text{eq}})} \tag{16}$$

where $D = \partial/\partial t + \mathbf{u} \cdot \partial/\partial \mathbf{x}$.

However, Eq. (16) is difficult to be used in the RTMC method directly due to the complexity of $D^2 f^{\text{eq}}/Df^{\text{eq}}$. Since Df^{eq} is both a temporal and spatial function, define $\mathfrak{I}(t, \mathbf{X})$ equal to Df^{eq} , then

$$\frac{D^2 f^{\text{eq}}}{Df^{\text{eq}}} = \frac{D(Df^{\text{eq}})}{Df^{\text{eq}}} = \frac{D\mathfrak{I}(t, \mathbf{X})}{\mathfrak{I}(t, \mathbf{X})} \tag{17}$$

where $\mathbf{X} = (x, y, z)$ is a spatial vector. Taking the x direction for example, Eq. (17) becomes,

$$\frac{D\mathfrak{I}(t, x)}{\mathfrak{I}(t, x)} = \frac{\partial\mathfrak{I}(t, x)/\partial t + u_x \partial\mathfrak{I}(t, x)/\partial x}{\mathfrak{I}(t, x)} \tag{18}$$

Eq. (18) consists of the time differential, $\partial\mathfrak{I}(t, x)/\partial t$, which denotes the relative difference between two time steps at a node and the space differential, $\partial\mathfrak{I}(t, x)/\partial x$, which denotes the relative difference between two nodes at the same time in the numerical calculation. Initially, $\partial\mathfrak{I}(t, x)/\partial t$ should be significant, but becomes negligible as the calculation is converged and $u_x \partial\mathfrak{I}(t, x)/\partial x$ becomes dominant. To simplify the generalized relaxation time and therefore, it can be easily used in RTMC method, we let,

$$\frac{\partial\mathfrak{I}(t, x)}{\partial t} + u_x \frac{\partial\mathfrak{I}(t, x)}{\partial x} \approx Au_x \frac{\partial\mathfrak{I}(t, x)}{\partial x} \tag{19}$$

that is, using the space term $Au_x \partial\mathfrak{I}(t, x)/\partial x$ to replace the sum of the time term $\partial\mathfrak{I}(t, x)/\partial t$ and space term $u_x \partial\mathfrak{I}(t, x)/\partial x$. When the calculation is going to converge, $u_x \partial\mathfrak{I}(t, x)/\partial x$ becomes dominant, the parameter A tends to 1.0. A is a parameter to be determined in the numerical simulation.

The local Knudsen numbers are defined as,

$$Kn_{L,x} = \frac{\lambda}{\rho} \left| \frac{\partial \rho}{\partial x} \right| \quad \text{and} \quad Kn_{L,y} = \frac{\lambda}{\rho} \left| \frac{\partial \rho}{\partial y} \right| \tag{20}$$

where ρ is the gas density, λ is the molecular mean free path, defined as $\lambda = 1/(\sqrt{2}\pi n d^2)$, n is the molecular number density and d is the molecular diameter. Using a dimensional analysis and the definition of Kn_L , Eqs. (16)–(20) can be combined to give the approximate expression

$$\tau \left(\frac{D^2 f^{\text{eq}}}{Df^{\text{eq}}} \right) = \tau \left(\frac{D\mathfrak{I}(t, x)}{\mathfrak{I}(t, x)} \right) \approx A \frac{\tau}{\lambda} u_x Kn_{L,x} \tag{21}$$

The similar result can be derived for the y direction. Therefore, the generalized relaxation time can be simplified as,

$$\tau^* = \frac{\tau}{1 + \tau(D^2 f^{\text{eq}}/Df^{\text{eq}})} \approx \frac{\tau}{1 + A \cdot \max \left(\frac{\tau}{\lambda} u_x Kn_{L,x}, \frac{\tau}{\lambda} u_y Kn_{L,y} \right)} \tag{22}$$

where u_x and u_y are the velocities in the x and y directions and $Kn_{L,x}$ and $Kn_{L,y}$ are the local Knudsen numbers in the x and y directions. The simplified generalized relaxation time is, therefore, related to the velocity, as expected [19].

3.4. Modified RTMC and its implement

In the modified RTMC method, the distribution function $f^{t+\Delta t}$ at time $t + \Delta t$ in the BGK model equation can be expressed as,

$$f^{t+\Delta t} = (g^*)^{t+\Delta t} - \frac{(\tau^*)^{t+\Delta t}}{(\tau^*)^t} \cdot ((g^*)^t - f^t) \quad (23)$$

where g^* is a generalized model, which can be the Maxwellian, ES and MTT models.

The calculational process for the modified RTMC method is

- (a) Initialize the program.
- (b) Move the particles taking into account the interactions between particles and boundaries.
- (c) Index the particles.
- (d) Sample and calculate the macro quantities in each cell; calculate the local Knudsen number by Eq. (20) and the simplified generalized relaxation time, τ^* , by Eq. (22).
- (e) Recalculate the particle velocities according to Eq. (23). The detail operation is: Generate a uniform random number $R_f(0)$. If $R_f(0) \leq (1 - \exp(-\Delta t/\tau^*))$ for any particle in a cell, then redistribute the velocities of the particles in that cell as following:
 1. Calculate the most probable velocity, V_m , according to the generalized model, g^* .
 2. Generate the random velocities of the particles (P_{V1} and P_{V2} in the program) by V_m .
 3. The redistributed velocities of the particles ($u^{t+\Delta t}$ and $v^{t+\Delta t}$) are composed with the random velocities (P_{V1} and P_{V2}) plus the macro velocities (U^t and V^t) at the last time step.
- (f) Return to (b) and continue the calculation until convergence.

In the modified RTMC method, the molecular collisions are modeled using the variable hard sphere (VHS) molecular model and the energy exchange between kinetic and internal energies is calculated by using the Larsen–Borgnakke model, in which a rotational collision number of $Zr = 5$ is fixed. The no-time-counter (NTC) scheme [1] is used in the present method. The time step, Δt , should be less than the mean collision time, so that the particle movement and their collisions are decoupled. Borrowing from the traditional computational fluid dynamics (CFD), this constraint may be expressed as a Courant–Friedrichs–Lewy (CFL) number, $CFL = c'_m \Delta t / \Delta x < 1$, where $c'_m = \sqrt{\gamma RT}$, is the most probable molecular speed, Δx is the cell size. The value of CFL is set at 0.25 in the present method.

4. Numerical experiments

4.1. Microchannel flow

The modified RTMC method was verified by simulating 2D gas flow in a microchannel for the physical model shown in Fig. 1. The length of microchannel was $L = 5 \mu\text{m}$, the height was $H = 1 \mu\text{m}$, $U_\infty = 200 \text{ m/s}$, was the freestream velocity, the freestream temperature was $T_\infty = 300 \text{ K}$ and the walls temperature was $T_w = 300 \text{ K}$. The grid had 50×10 cells with 4×12 sub-cells in each cell, the time step was $7.08 \times 10^{-11} \text{ s}$, the Knudsen number was 0.1 using the microchannel height as the characteristic length, the initial number density was 1.29×10^{25} . The variable hard sphere (VHS) molecules and the diffuse reflection model were used both in the modified RTMC and DSMC methods for all the simulations. The parameter A was equal to 1.0 in the simplified generalized relaxation time. The total molecule number was 42,111, the total number of samples was 788,020. The working gas was nitrogen for all the simulations. Table 1 listed the properties of N_2 .

The numerically calculated velocity, density and pressure distributions along the centerline of the microchannel are shown in Figs. 2–4 for $Kn = 0.1$. The distributions were calculated using the modified RTMC with

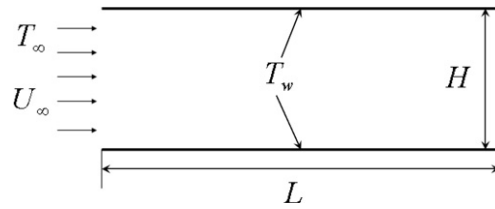


Fig. 1. Schematic of microchannel flow.

Table 1
Properties of N_2

m (kg)	ζ	d_{ref} (m)	T_{ref} (K)	ω
4.65E-26	2	4.17E-10	273	0.74

the Maxwellian, ES and MTT models, with DSMC results also plotted for comparison. The velocity based on the Maxwellian distribution is lower than that given by the DSMC in the inlet section (Fig. 2). The probable reason is the unity Pr , which can not predict the real ratio between the momentum and heat transfer diffusion rates. However, although Pr is taken as 0.72 in the ES model, the velocity still has differences at the inlet and outlet sections from the DSMC results. The differences with $Pr = 0.72$ are obvious, especially for the density and pressure comparisons in Figs. 3 and 4. Inaccurate values of $\beta_{11} = RT/Pr$, $\beta_{22} = \alpha RT/(1 + \alpha)$ and $\alpha = 1$ in the ES model may affect the simulation results, which requires further analyses in the future.

The MTT model gives more accurate results than Maxwellian and ES models as shown in Figs. 2–4 with the numerical predictions of the modified RTMC with the MTT model being more consistent with the DSMC results. The more accurate results are not only due to the flow variables in the MTT model being updated based on the mass, momentum, and energy conservation through the fluxes on the macroscopic level, but also the fluxes are constructed on the microscopic level based on the gas-kinetics equation [15].

The parameter A introduced in the process of simplifying the generalized relaxation time is very difficult to be determined analytically. At the beginning of numerical calculation, $\partial \mathfrak{S}(t, x)/\partial t$ is more significant than $u_x \partial \mathfrak{S}(t, x)/\partial x$, the parameter A can be larger or smaller than 1.0 in Eq. (19). To study the effect of parameter A on the numerical results, three values of A , 10^3 , 1.0 and 10^{-3} , were checked in the simulation.

Figs. 5–7 show the velocity, density and pressure distributions along the centerline of the microchannel for the three values of A using the MTT model. The results indicate that the velocities agree well with the results by DSMC method for all the values of A , while some disagreement in the inlet section are shown in the Fig. 7 for the pressures. However, the Fig. 6 shows the obvious difference of densities when A equals 1000 against the

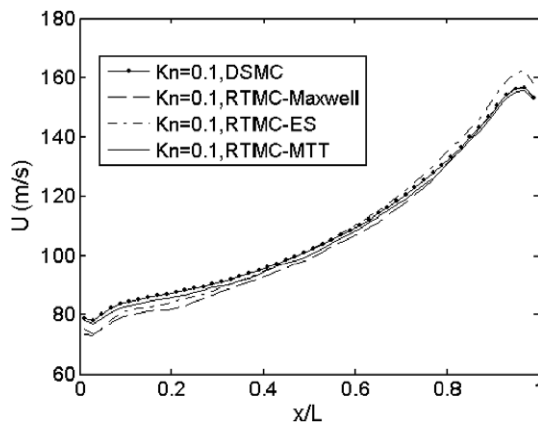


Fig. 2. Velocity distributions along the centerline of the microchannel predicted by the modified RTMC for $Kn = 0.1$.

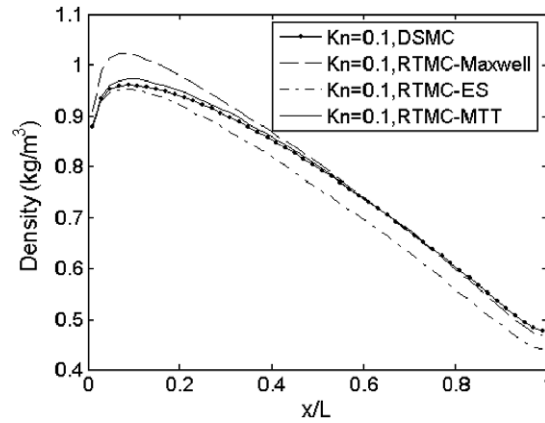


Fig. 3. Density distributions along the centerline of the microchannel predicted by the modified RTMC for $Kn = 0.1$.

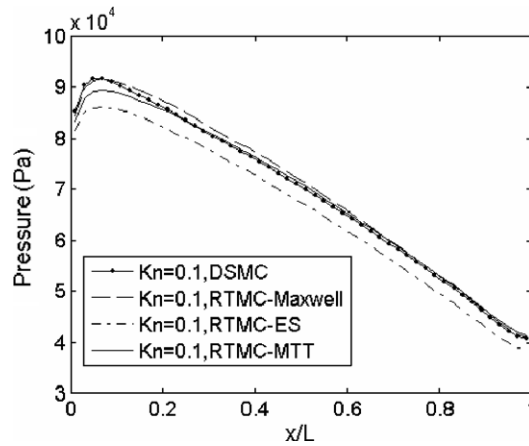


Fig. 4. Pressure distributions along the centerline of the microchannel predicted by the modified RTMC for $Kn = 0.1$.

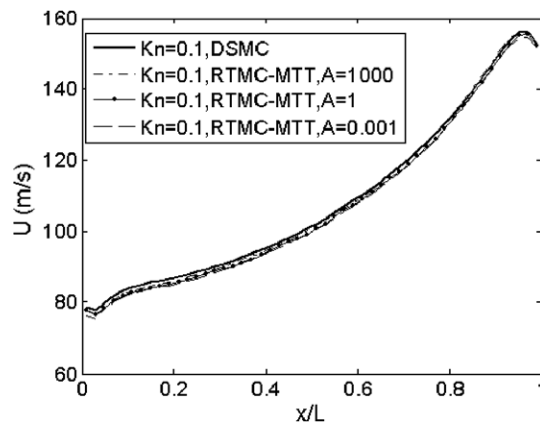


Fig. 5. Velocity distributions along the centerline in a microchannel for various A .

other two small values of A . Therefore, the current paper proposes that a fitting A in the simplified form of the generalized relaxation time should be smaller than 1.0 for the accurate numerical results of the gas flow in the microchannel for $Kn = 0.1$.

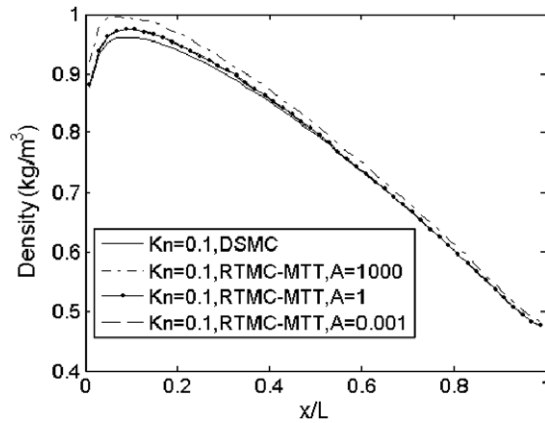


Fig. 6. Density distributions along the centerline in a microchannel for various A .

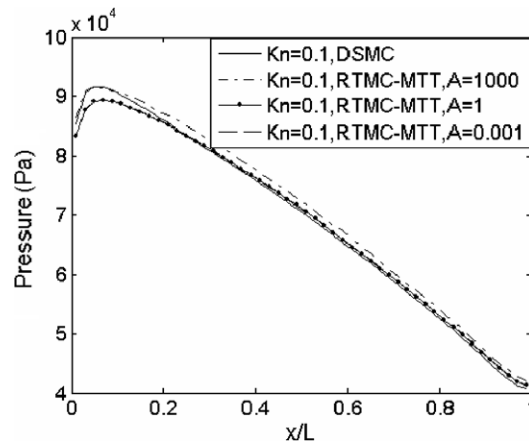


Fig. 7. Pressure distributions along the centerline in a microchannel for various A .

The gas density strongly affects the computational cost of DSMC method due to the frequent particle collision and sampling. However, the computational cost of the modified RTMC is relative to the macro-information statistic for local Knudsen number and the velocity redistribution of the particles which are sampled based on the simplified generalized relaxation time. For the cases with small Kn , the computation cost of RTMC is less than DSMC. For the microchannel gas flow shown in Fig. 1, the modified RTMC with the MTT model is about 64% cost of the DSMC method for $Kn = 0.1$, when the costs of both the methods are on a same level for $Kn = 1.0$. With the Knudsen number decreases, the costs of the present method is about 57% for $Kn = 0.05$ and 43% for $Kn = 0.01$ of those of DSMC method, respectively.

4.2. Couette flow in microchannels

Beskok [20] presented an analytical solution for the velocity distribution for micro-Couette flows by introducing second order slip boundary conditions. The velocity distribution for micro-Couette flow [9] is

$$\frac{u}{U_0} = \left(\frac{y}{H} + \frac{2 - \sigma_v}{\sigma_v} Kn \right) / \left(2 \times \frac{2 - \sigma_v}{\sigma_v} Kn + 1 \right) \tag{24}$$

where U_0 is the upper plate velocity, H is the distance between the two plates and σ_v is the momentum accommodation coefficient.

The expression for the dimensionless temperature [9] is

$$\frac{T - T_w}{T_g - T_w} = \left(-\left(\frac{y}{H}\right)^2 + \frac{y}{H} + \frac{2 - \sigma_T}{\sigma_T} \frac{2\gamma}{\gamma + 1} \frac{Kn}{Pr} \right) / \left(\frac{2 - \sigma_T}{\sigma_T} \frac{2\gamma}{\gamma + 1} \frac{Kn}{Pr} \right) \tag{25}$$

where T_w is the plate temperature, T_g is the gas temperature near the plate, σ_T is the thermal accommodation coefficient.

The micro-Couette flow was simulated using the modified RTMC with the MTT model. To reduce the computational cost, periodic and fully developed boundary conditions were used at the inlet and outlet. The simulation region shown in Fig. 8 was $1 \times 1 \mu\text{m}$, the grid had 50×50 cells with 2×2 sub-cells in each cell, the velocity of the upper plate U_0 was 300 m/s, the temperatures of both the upper and lower plates were 300 K and the inlet and outlet pressures were the standard values. “M” denotes macro quantities, such as pressure and temperature. The three simulations had Knudsen numbers of 0.129, 0.0646 and 0.0482, with number densities of 1.0×10^{25} , 2.0×10^{25} and 2.687×10^{25} . The time step was 9.93×10^{-12} s for three Knudsen numbers. The total molecule number was over 25,000, and the total number of samples was over 400,000. In the analytical solutions, $\sigma_v = 1.0$, $\sigma_T = 1.0$, $\gamma = 1.4$ and $Pr = 0.72$.

The dimensionless velocities for the three Knudsen numbers predicted by the modified RTMC with the MTT model agree well with the analytical solutions as shown in Fig. 9. The results show that the slip velocity near the plate increases with increasing Kn . When $Kn = 0.0646$, the numerically predicted slip velocity at the wall is 20.4 m/s, while the slip velocity is 16.8 m/s for $Kn = 0.0482$, which is about half of the result for $Kn = 0.129$. From Eq. (24), the slip velocity can be written as

$$\frac{u_s}{U_0} = \frac{2 - \sigma_v}{\sigma_v} / \left(2 \times \frac{2 - \sigma_v}{\sigma_v} + \frac{1}{Kn} \right) \tag{26}$$

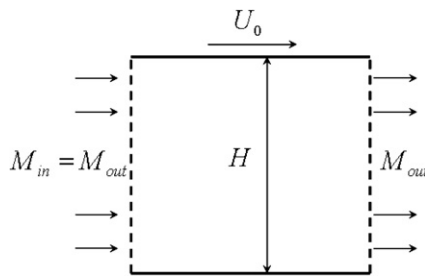


Fig. 8. Micro-Couette flow with periodic boundary conditions.

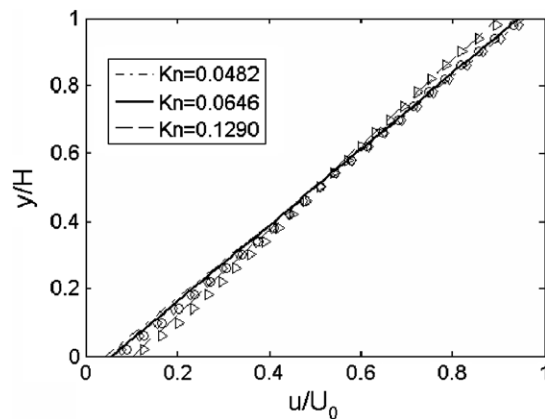


Fig. 9. Dimensionless velocity distributions for micro-Couette flow for various Kn .

where u_s is the slip velocity. Thus, the slip velocity is directly proportional to the Knudsen number as seen in the Table 2.

Fig. 10 shows that the dimensionless temperature distributions along the y direction are almost identical with the analytical solutions. The differences between the numerical results and analytical solutions result from the statistical noise.

4.3. Poiseuille flow in microchannels

For micro-Poiseuille flow, the first-order analytical solution for the velocity [9] is:

$$\frac{u}{u_c} = \left[-\left(\frac{y}{H}\right)^2 + \frac{y}{H} + Kn \right] / \left(\frac{1}{4} + Kn \right) \tag{27}$$

where u_c is the local velocity at the centerline and H is the microchannel height.

The simulation region was $5 \times 1 \mu\text{m}$ for the micro-Poiseuille flow simulations. The grid had 50×20 cells with 4×4 sub-cells in each cell, the inlet pressure was $P_{\text{in}} = 1.5 \times 10^5 \text{ Pa}$ and the outlet pressure was $P_{\text{out}} = 1.0 \times 10^5 \text{ Pa}$, the walls temperature was 300 K. The three simulations had number densities of 1.0×10^{25} , 2.0×10^{25} and 3.62×10^{25} , with the corresponding Knudsen numbers defined using the height H being 0.129, 0.0647 and 0.0357. The time step was $1.13 \times 10^{-10} \text{ s}$ for three Knudsen numbers. The total molecule number was over 21,000 and the total number of samples was over 890,000.

To improve convergence, the characteristic pressure boundary conditions [21] were used at the inlet and outlet. Fig. 11 shows the dimensionless velocities. The numerical results are in good agreement with the analytical solutions for the various Knudsen numbers. The results verify that the modified RTMC with the MTT model can accurately simulate continuum-transition gas flows in microchannels.

Table 2
Analytical and numerical slip velocities for various Kn for micro-Couette flows

Kn	Slip velocity (m/s)	
	Analytical	Numerical
0.0482	13.15	16.88
0.0646	17.16	20.35
0.129	30.82	31.97

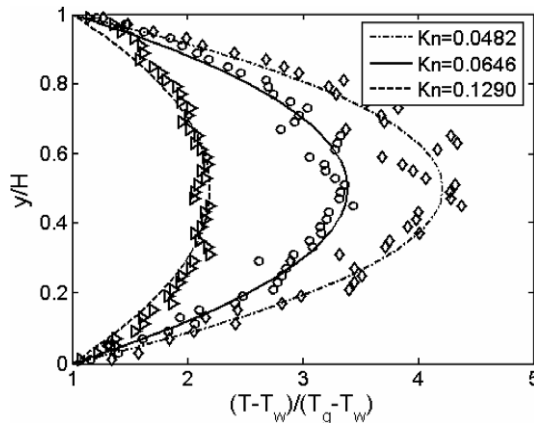


Fig. 10. Dimensionless temperature distributions for micro-Couette flow for various Kn .

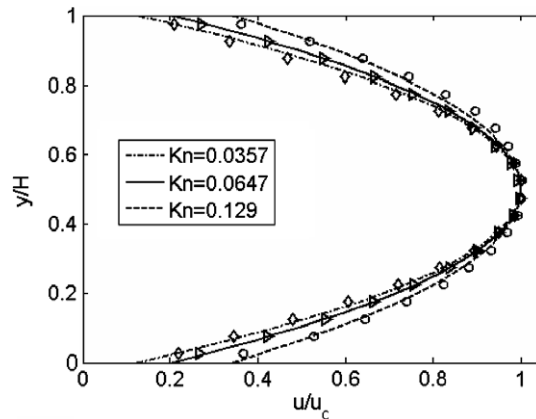


Fig. 11. Dimensionless velocity distributions for micro-Poiseuille flow for various Kn .

5. Conclusion

The relaxation time Monte Carlo (RTMC) method was modified by introducing the Maxwellian, ES, or MTT models into the BGK model equation to accurately simulate continuum-transition flows. A simplified form of the generalized relaxation time, which is related to the macro velocities and the local Knudsen number, was developed to be used in the modified RTMC method. The results of the microchannel gas flow simulations using the modified RTMC with the MTT model are better than those with the other two models (Maxwellian model and ES model) and agree well with the DSMC method results. The numerical results for micro-Couette flow and micro-Poiseuille flow for various Knudsen numbers predicted by the modified RTMC method are in good agreement with the analytical solutions. The computational time consumed by the modified RTMC with the MTT model is less than that of the DSMC for continuum-transition simulation; thus, the modified RTMC method is more efficient than the DSMC method for continuum-transition gas flow simulations and lays the foundation for a hybrid method in the future.

Acknowledgment

This work was supported by the Tsinghua National Laboratory for Information Science and Technology, China.

References

- [1] G.A. Bird, *Molecular Gas Dynamics and the Direct Simulation of Gas Flows*, Clarendon Press, 1994.
- [2] G.E. Karniadakis, A. Beskok, *Micro Flows: Fundamentals and Simulation*, Springer, 2002.
- [3] C.T. Ying, *Gas Transport Theory and Application*, Tsinghua University Press, Beijing, 1990.
- [4] D.I. Pullin, Direct simulation methods for compressible inviscid ideal-gas flow, *J. Comput. Phys.* 34 (1980) 231.
- [5] W.F. Chen, M.Q. Wu, B. Ren, On study of hybrid DSMC/EPsm method, *Chinese J. Comput. Mech.* 20 (2003) 274.
- [6] M.N. Macrossan, A particle simulation method for the BGK equation, in: T. Bartel, M. Gallis (Ed.), *Rarefied Gas Dynamics Proceedings of the 22nd International Symposium*, Sydney, Am. Inst. Phys., NY 2001, p. 426.
- [7] M.N. Macrossan, v-DSMC: A fast simulation method for rarefied flow, *J. Comput. Phys.* 173 (2001) 600.
- [8] M.N. Macrossan, μ -DSMC: A general viscosity method for rarefied flows, *J. Comput. Phys.* 185 (2003) 612.
- [9] M.R. Wang, Monte Carlo simulation on micro- and nanoscale gas flow and heat transfer, Ph.D. thesis, Tsinghua University, 2004.
- [10] M.R. Wang, M.N. Macrossan, Z.X. Li, Relaxation time simulation method with internal energy exchange for perfect gas flow at continuum-transition region, *Commun. Nonlinear Sci. Numer. Simulation* 12 (2007) 1277.
- [11] L.H. Holway, New statistical models for kinetic theory: methods of construction, *Phys. Fluids* 9 (1966) 1658.
- [12] X.W. Zhang, S.G. Hu, C.J. Zhang, On the spatially homogeneous ES model of the Boltzmann equation, *Math. Appl.* 19 (2) (2006) 426.
- [13] K. Xu, E. Josyula, Multiple translational temperature model and its shock structure solution, *Phys. Rev. E* 71 (2005) 056308.
- [14] K. Xu, H.W. Liu, Multiple-temperature kinetic model for continuum and near continuum flows, *Phys. Fluids* 19 (2007) 016101.

- [15] K. Xu, H.W. Liu, Multiscale gas-kinetic simulation for continuum and continuum-transition flows, *Phys. Rev. E* 75 (2007) 016306.
- [16] H. Grad, On the kinetic theory of rarefied gases, *Pure Appl. Math.* 5 (1949) 325.
- [17] H.M. Mott-Smith, The solution of the Boltzmann equation for a shock wave, *Phys. Rev.* 82 (1952) 885.
- [18] A. Bird G, Direct simulation of the Boltzmann equation, *Phys. Fluids* 13 (1970) 2676.
- [19] P.L. Bhatnagar, E.P. Gross, M.A. Krook, Model for collision processes in gases. I. Small amplitude processes in charged and neutral one-component systems, *Phys. Rev.* 94 (3) (1954) 511.
- [20] A. Beskok, Simulation and models for gas flows in microgeometries, Ph.D. thesis, Princeton University, 1996.
- [21] M.R. Wang, J.K. Wang, Z.X. Li, New implement of pressure boundary conditions for DSMC, *Chinese J. Comput. Phys.* 21 (4) (2004) 316.